Advanced MRI

Phase Difference Reconstruction

Faik Can MERAL

Outline

- Introduction
- Quantitative Description
  - Arctangent operation
  - ATAN2
- Phased-Array Multiple Coil Data
- Correction of Predictable Phase Errors and the Concomitant Field
- Image Warping
- Image Scaling
- Noise Masking

Introduction

- MRI is a phase sensitive imaging modality
- Each pixel has a magnitude and phase data (complex nature of the MR signal). When standard magnitude reconstruction is performed phase information is superimposed within the magnitude information.
- Information encoded in phase data
  - Bo homogeneity: used for Shimming
  - Fluid Flow: phase contrast angiography
  - MR temperature mapping
  - MR elastography

Introduction

- In MR acquisitions there are invariably unwanted contributions to the image phase.
  - System imperfections:
    - Gradient eddy currents
  - Unavoidable physical effects:
    - Chemical shift
    - Magnetic susceptibility variations
    - Concomitant field
- It is more difficult to interpret this phase map due to the unwanted phase.
- Two sets of acquisitions are made and a phase difference map is formed to address this problem.

Introduction

- Phase Difference Map: Difference between a pair of phase images on a pixel-by-pixel basis.
- The goal is to obtain the desired phase while eliminating the unwanted phase.

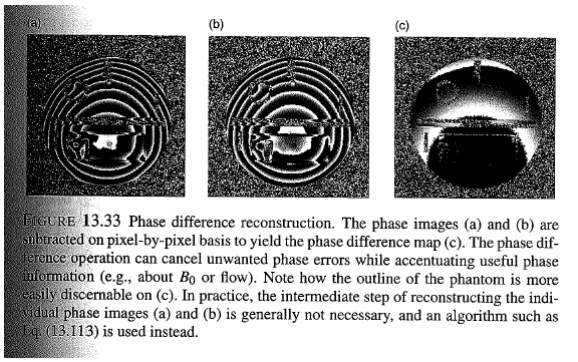

FIGURE 13.33 Phase difference reconstruction. The phase images (a) and (b) are subtracted on pixel-by-pixel basis to yield the phase difference map (c). The phase difference operation can cancel unwanted phase errors while accentuating useful phase information (e.g., about B_0 or flow). Note how the outline of the phantom is more easily discernable on (c). In practice, the intermediate step of reconstructing the individual phase images (a) and (b) is generally not necessary, and an algorithm such as Eq. (13.113) is used instead.

i.e. to produce a Bo map for shimming, two Gradient Echo data sets are acquired with identical parameters, except TE is varied. Difference of these two images gives the phase difference map.
i.e. in phase-contrast angiography: flow encoding gradient is modified between the two acquisitions and a phase diff map is reconstructed.

Quantitative Description

- Pixel-by-pixel arctangent operation
  - Output is defined in the interval $-\pi/2 < \arctan(x) < \pi/2$
  - Any values outside the primary range are represented by a value in the primary range (alias)
  - Aliasing in the phase map is accompanied by discontinuities called phase wraps

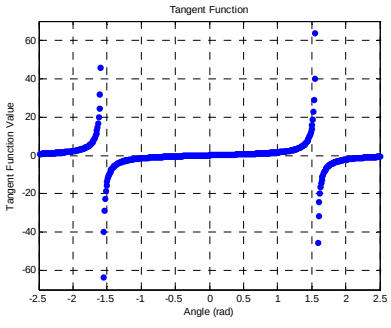

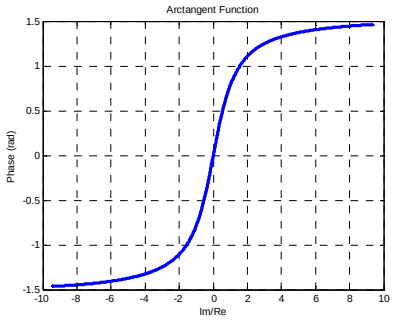

Quantitative Description

- Two k-space acquisitions to obtain a phase difference map
- The complex nature of MR signal
  - For a particular pixel on image 1➔ $z_1 = x_1 + iy_1 = \rho_1 e^{i\phi_1}$
    and image 2➔ $z_2 = x_2 + iy_2 = \rho_2 e^{i\phi_2}$

$$\Delta\phi = \phi_1 - \phi_2 = phase(z_1) - phase(z_2) = \arctan(\frac{y_1}{x_1}) - \arctan(\frac{y_2}{x_2})$$

- For computational efficiency and to minimize phase wraps, an optimal phase difference reconstruction should employ only a single arctangent operation per pixel, because two arctangent operations are computationally costly and introduce extra phase wraps.

$$\Delta\phi = \arg(\frac{z_1}{z_2}) = \arg(\frac{\rho_1 e^{i\phi_1}}{\rho_2 e^{i\phi_2}}) = \arg(\frac{\rho_1}{\rho_2} e^{i(\phi_1 - \phi_2)}) = \arctan(\frac{\mathrm{Im}(z_1/z_2)}{\mathrm{Re}(z_1/z_2)})$$

- Since complex conjugate and the inverse of a complex number z_2 both have same phase

$$\Delta\phi = \arg(z_1 z_2^{*}) = \arg(\rho_1 e^{i\phi_1} \rho_2 e^{-i\phi_2}) = \arg(\rho_1 \rho_2 e^{i(\phi_1 - \phi_2)}) = \arctan(\frac{\mathrm{Im}(z_1 z_2^{*})}{\mathrm{Re}(z_1 z_2^{*})})$$

Quantitative Description

- Four Quadrant ATAN2 function: “ATAN2(input1,input2)”
  - ATAN2 runs a test to check the sign of individual argument before forming their ratio

i.e. num➔(+) & den➔(+), the phase lies in the 1st quadrant
num➔(+) & den➔(-), ……2nd quadrant
num➔(-) & den➔(-), ……3rd quadrant
num➔(-) & den➔(+), ……4th quadrant

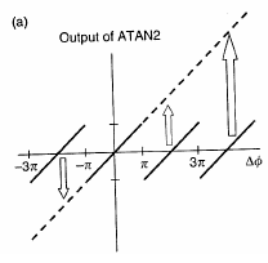

• Thus the actual range of conventional arctangent function [$-\pi/2$, $\pi/2$] is extended to [$-\pi$, π]
• Still any phase difference value lies outside the primary range [$-\pi$, π] will be aliased back in primary range. The true values can be obtained by adding or subtracting the multiples of 2π (phase unwrapping)
• Additional advantage of ATAN2 function is instead of reporting a divide-by-zero error when the second argument is zero it returns the correct value of $-\pi/2$, $\pi/2$

Phase Arranged Multiple Coil Data

- Many acquisitions use multiple coils arranged in a phased array.
- Optimal acquisition and processing of these data requires multiple receiver coils
- Using an algorithm a phase difference map can be reconstructed from this multichannel data.

$$\Delta\phi = \arg(\sum_j \frac{z_1 z_2^*}{\sigma_j^2}) = ATAN2(\mathrm{Im}\sum_j \frac{z_1 z_2^*}{\sigma_j^2}, \mathrm{Re}\sum_j \frac{z_1 z_2^*}{\sigma_j^2})$$

where σ_j^2 is the measured noise variance for the j^{th} channel

Phase Arranged Multiple Coil Data

Example: suppose $\Delta\phi$ is near the aliasing boundary π and there are 2 receiver channels . Because of noise

$\Delta\phi_1 = \pi - \varepsilon$

$\Delta\phi_2 = -\pi + \varepsilon$

Averaging these two phase gives simply zero. However if the multiple-receiver combination is made before the arctangent operation

$$\Delta\phi = \arg(z_1 z_2^*) = \arg(\sum \frac{\rho_{1j}\rho_{2j}e^{i\Delta\phi_j}}{\sigma_j^2})$$

Assume the noise variance and image magnitudes have only weak dependence on the index j, so we can remove ρ and σ

$$= \arg(e^{i(\pi-\varepsilon)} + e^{i(-\pi+\varepsilon)}) = \arg(e^{i\pi}(e^{-i\varepsilon} + e^{-2\pi i}e^{i\varepsilon}))$$

$$= \arg(e^{i\pi} 2\cos\varepsilon) = \pi$$

Correction of Predictable Phase Errors & The Concomitant Field

- After forming phase difference image, there are still unwanted phase errors
  - Phase contamination due to gradient eddy currents that can plague phase contrast angiography. Eddy currents are hardware dependent, so it is not very easy to predict the phase error in advance
  - However the constant and linear phase could be determined with a polynomial fit of the phase difference image where there should be no phase difference, such as stationary tissue in phase contrast angiogram.
    - Since the fitted phase is due entirely system imperfections, this can then be removed by post processing.

Correction of Predictable Phase Errors & The Concomitant Field

- Phase errors such as the one produced by concomitant field can be predicted with accuracy.
  - In that case it is advantageous to correct these phase errors before calculating the arctangent.
  - This avoids phase wraps in the phase difference map, and reduce the need for later phase unwrapping.
- Concomitant field has nonlinear spatial dependence, removing its phase error at this stage makes it easier to fit the eddy-current phase errors later.

Correction of Predictable Phase Errors & The Concomitant Field

- If the calculated concomitant field error at the pixel of interest is ϕ_e, then the phase corrected version is

$$\Delta\phi_{corr} = \arg(z_1 z_2^{*} e^{-i\phi_e}) = ATAN2[\mathrm{Im}(z_1 z_2^{*} e^{-i\phi_e}), \mathrm{Re}(z_1 z_2^{*} e^{-i\phi_e})]$$

- For multiple coil case: the phase error from the concomitant field is independent of the receiver channel number, the phase correction for multiple coil case.

$$\Delta\phi_{corr} = \arg(e^{-i\phi_e} \sum_j \frac{z_{1j} z_{2j}^{*}}{\sigma_j^2})$$

For further information on “Predictable Phase Errors and The Concomitant Field Phase Correction” refer to the journal article by Bernstein et al.1998

Image Warping

- Image warping operation can be applied to phase difference images.
- MRI is based on the assumptions of
  - linear gradients,
  - homogenous Bo fields
  - no concomitant gradient fields
  - no eddy-currents
- These are effects those diverge MRI from the ideal.

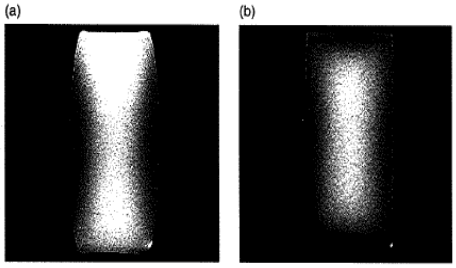

- The resultant image is distorted both in size and intensity
- In 2D slice selection the slice location is also shifted and is not planar. (potato chip effect)
- Measurement and correction of the various distortions are referred in the studies of Langlois (1997) and Hajnal (2001)

Image Warping

- It is preferable to apply image warping prior to arctangent.
  - Since image warping is a conformal mapping that uses interpolation methods such as cubic splines, it may introduce phase wraps if applied after arctangent, and the sharp discontinuities can cause unwanted ringing in the image.
  - Also a phase difference image processed in this way cannot be properly unwrapped later, because the sharp transition between $-\pi$ and $+\pi$ has been distorted.
- If warping operation is indicated by function W

$$\Delta\phi_{warped} = \arctan\left(\frac{W(\mathrm{Im}(z_1 z_2^{*}))}{W(\mathrm{Re}(z_1 z_2^{*}))}\right) = ATAN2[W(\mathrm{Im}(z_1 z_2^{*})), W(\mathrm{Re}(z_1 z_2^{*}))]$$

W should be on the entire image, not on a single pixel

- Again applying W before ATAN2 and separately to the real and imaginary images is advantageous because any change in image intensity caused by the warping algorithm will not effect the phase difference map.

Image Scaling

- The output of the ATAN2 function is real in the range of $-\pi$ and $+\pi$. sometimes we want to scale this output to a more convenient range by multiplying it by some constant.

i.e.

In phase contrast angiography, the output can be scaled so that the pixel values represent velocity in convenient units such as millimeter per second.

For Bo mapping, the pixel intensity may represent the frequency offset δf in Hertz, tenths of Hertz or ppm.

Example

Suppose Bo map is obtained by forming the phase difference from the two GRE images with values of TE equal to 10ms and 25ms. How should the result of the phase difference map be scaled so that each intensity count represents a frequency offset of 0.1 Hz?

Solution: phase in radians $\Delta\phi$ ➔ frequency δf

$$\delta \mathrm{f}\left[\frac{\mathrm{Hz}}{10}\right] = \frac{10\Delta\phi}{2\pi\Delta\mathrm{TE}} = \frac{10\Delta\phi}{2\pi(0.025s - 0.010s)} = 106.1\Delta\phi$$

Noise Masking

- Noise
  - Standard magnitude image➔ 
  - Phase difference image ➔ 
- Masking methods
- Threshold: a magnitude image is reconstructed from same data. M: the magnitude image corresponding to the phase difference map.

$$M = \sqrt{\left| \sum_j \frac{z_1 z_2^*}{\sigma_j^2} \right|}$$ (for multiple coil case)

- Then the phase difference map can be masked

$$\Delta\phi_{thresh} = \begin{cases} \Delta\phi & M \geq M_0 \\ 0 & M < M_0 \end{cases}$$

- Multiplication: multiply the phase difference image by the magnitude image on a pixel by pixel basis.

$$\Delta\phi_{mult} = M\Delta\phi$$

Noise Masking

- Both methods have their advantages and disadvantages.
- The threshold method:
  - Phase difference pixel values are not altered, still some quantitative information can be found in the data
  - Over-aggressive method so can zero out interested pixel values. Finding proper threshold needs operator intervention.
- The multiplication method:
  - All pixel values are retained.
  - The masked data must be divided by the mask in order to obtain true phase difference information.

Phase Difference Reconstruction

- Summary

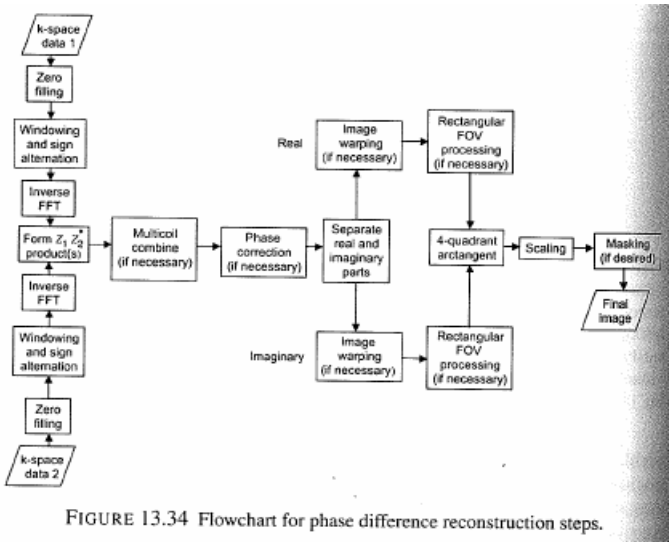

FIGURE 13.34 Flowchart for phase difference reconstruction steps.

Advanced MRI

Magnetic Resonance Elastography (MRE)

by

Faik Can Meral

Outline

- Introduction
  - Elasticity
  - Acoustics
- Theory
  - MRE pulse sequence
  - Reconstruction of Elastic Properties
- Experimental Studies
  - MRE Setup
  - Results
- Recent & Future Work

Introduction

- Palpation: the stiffness of the tissue, particularly its resistance to pressure and shear forces, is inspected by hand.
- i.e. cancerous tissue can be detected, since it appears as a hard lesion, due to the increased stromal density
- Even for some tasks palpation can be more sensitive than imaging, however it is subjective and limited to the hand accessible abnormalities

- Question: Can there be an imaging modality to quantitatively map the mechanical properties of human tissue?

Introduction

- **Problem definition:**
  - Creation of a technology for measuring the mechanical properties of tissue that provides beneficial information about the characterization of the tissue.
- **Mechanical Properties:**
  - Young's Modulus
  - Shear Modulus: span a large dynamic range and provide significant contrast between normal and abnormal tissues
  - Bulk Modulus

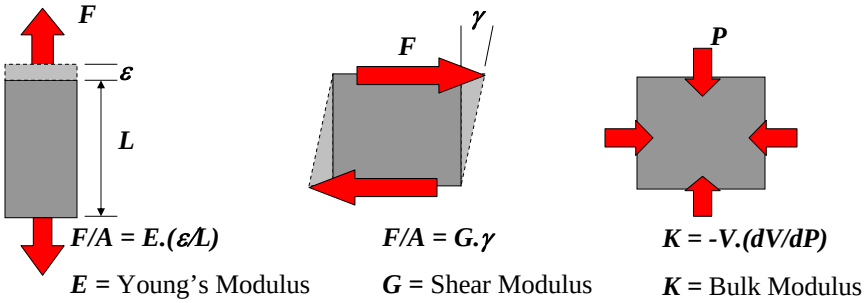

$F/A = E.(\varepsilon/L)$ — E = Young's Modulus

$F/A = G.\gamma$ — G = Shear Modulus

$K = -V.(dV/dP)$ — K = Bulk Modulus

Introduction

- **Solution:**
  - **Method:** Quantitatively mapping the physical response of a material to harmonic mechanical excitation allows calculation of regional mechanical properties such as shear modulus.
  - **Ultra-Sound Elastography:** Doppler effect is used to provide localized information about tissue motion to map shear wave propagation at lower excitation frequencies (20 – Several Hundred Hertz)
  - **MR Elastography:** A phase contrast based MRI technique with high sensitivity to cyclic displacement that is capable of quantitatively imaging low frequency transverse acoustic strain waves in tissue like materials.

Introduction

- Vibration & Acoustics:
  - Wave dynamics in solids: Vibrations
  - Wave dynamics in fluids or viscous media: Acoustics

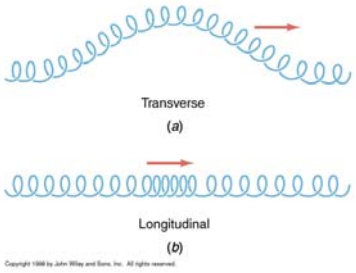

  - Energy is transferred by waves
  - Two types of waves
    - Longitudinal (Compression)
    - Transverse (Shear)

Question: Why are we dealing with shear (transverse) waves instead of compression (longitudinal) waves?

Introduction

- Elastography:
  - MRE:
    - Relatively low magnetic fields in clinical MRI systems (1.5 Tesla)
    - Typical voxel resolution 1mm x 1mm x 10mm
  - μMRE:
    - Basic principals are extended to high resolution MR systems (10 Tesla)
    - Voxel resolution 34μm x 34μm x 500μm
    - Shear wave images at 550 ~ ? Hz can be acquired

Theory

$$\phi = \gamma \int^{\tau} \vec{G}_r(t).\vec{r}(t)dt$$

- The phase equation in the presence of magnetic field gradient.

$$\vec{r}(t) = \vec{r}_0 + v_0.t$$

- A simple linear motion of r(t) with a constant velocity

$$\mathbf{r}(t) = \mathbf{r}_0 + \vec{\xi}(\mathbf{r},t)$$

$$\vec{\xi}(\mathbf{r},\boldsymbol{\theta}) = \vec{\xi}_0.\cos(\mathbf{k}.\mathbf{r} - \omega t + \boldsymbol{\theta})$$

- However, if the duration of the motion is smaller than the echo time or if the trajectory of motion is complicated, in our case: propagating harmonic acoustic strain wave so the spins are making a harmonic motion about their mean position

- The gradient $G_r(t)$ is switched in polarity at the same frequency as the nuclear spin motion (ω_{spin})

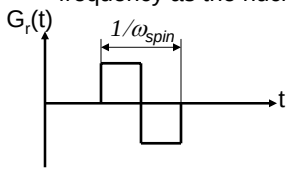

$$\int_0^{\tau} \vec{G}_r(t)dt = 0$$

Theory

- Then the accumulated phase becomes

$$\phi(\mathbf{r},\boldsymbol{\theta}) = \gamma \int_0^{\tau=NT<TE} \vec{G}_r(t).\vec{\xi}_0.\cos(\mathbf{k}.\mathbf{r} - \omega t + \boldsymbol{\theta})dt$$

$$= \frac{2\gamma NT(\mathbf{G}_\mathbf{r}.\vec{\xi}_0)}{\pi}.\sin(\mathbf{k}.\mathbf{r} + \boldsymbol{\theta})$$

k: the wave number

ξ_0: peak displacement of the spin from the mean position

ω: acoustic excitation frequency

θ: initial phase offset (between the bipolar gradient and the acoustic waves)

N: number of gradient cycles

T: period of gradient cycles

- Above equation shows that the measured phase shift is proportional to the scalar product of the displacement vector and the gradient vector and to the period and the number of gradient cycles.

Theory

- Two phase measurements are made by toggling the bipolar gradient pulses, positive to negative.
- The phase images are calculated and subtracted to get the phase difference map which corresponds to the shear wave image.
- The MR received phase shift is collected using a phase contrast gradient or spin echo pulse sequence.
- Magnitude of the detected phase can be increased by using multiple number of bipolar gradient pulses.

Theory

- Reconstruction of Elastic Properties from phase information:
  - Voigt Model is used to represent the tissue.
    - spring & damper in parallel
  - The visco-elastic parameters can be reduced to two complex constants: Lame constants.

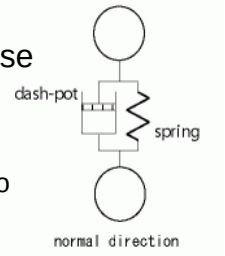

$\lambda = \lambda_1 + j\omega\lambda_2$ volume elasticity, volume viscosity

$\mu = \mu_1 + j\omega\mu_2$ shear elasticity, shear viscosity

- For soft biological tissues $\mu_1 << \lambda_1$, $\lambda_1 = 2.6$ GPa and $\lambda_2 = 0$ (for the interested frequency range)
- Other elastic properties such as Young's Modulus, Poisson's Ratio can be expressed in terms of these constants.

Theory

- Shear wave information such as wavelength (λ_s), logarithmic decrement (δ) and frequency (f) can be obtained from experimental results.
- Those are related to μ_1 and μ_2 with the given equations.

$$c_s = \sqrt{\frac{2}{\rho}\frac{\mu_1^2 + (2\pi f)^2\mu_2^2}{\mu_1 + \sqrt{\mu_1^2 + (2\pi f)^2\mu_2^2}}} \qquad \lambda_s = \frac{1}{f}\sqrt{\frac{2}{\rho}\frac{\mu_1^2 + (2\pi f)^2\mu_2^2}{\mu_1 + \sqrt{\mu_1^2 + (2\pi f)^2\mu_2^2}}}$$

$$\delta = \frac{4\pi^2 f\mu_2}{\mu_1 + \sqrt{\mu_1^2 + (2\pi f\mu_2)^2}}$$

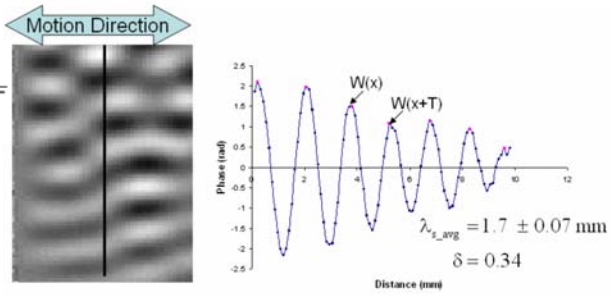

Experimental Studies

- Agar Gel Phantom: different types of tissues are simulated by different amount of agarose solved in water (0.1%~3.0%)
- Some real tissue experiments are done.
  - Porcine kidney (Ehman et al. 1995)
  - Bovine muscle (Felmlee et al. 2000)
  - Frog oocytes & MSCs (Othman et al. 2005)
- But most of the literature available is on gel phantom experiments.

Experimental Studies

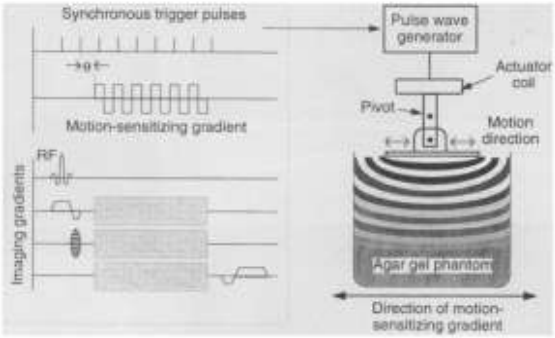

Fig. 1. Experimental system for observing acoustic strain waves with MRI. A gradient-echo imaging pulse sequence was modified to incorporate a gradient wave form for sensitizing the sequence to harmonic motion and to generate synchronous pulses for triggering the motion of an electromechanical actuator. The actuator consists of an electrical coil attached to a pivot bar and is driven by a wave generator at 50 to 1000 Hz. The alternating flux of the coil interacts with the main magnetic field of the imager, yielding a cyclic force, which is coupled by a contact plate to the surface of the object to be studied. The period and the number of motion-sensitizing gradient pulses are adjustable, as is the phase relation (ϕ) between the cyclic gradient wave form and the trigger pulses. An adjustable number of trigger pulses can be applied before the initial radio frequency (RF) excitation to establish a mechanical steady state. The motion-sensitizing gradients can be applied along any desired axis (indicated by shaded regions) in combination with the imaging gradients.

Experimental Studies

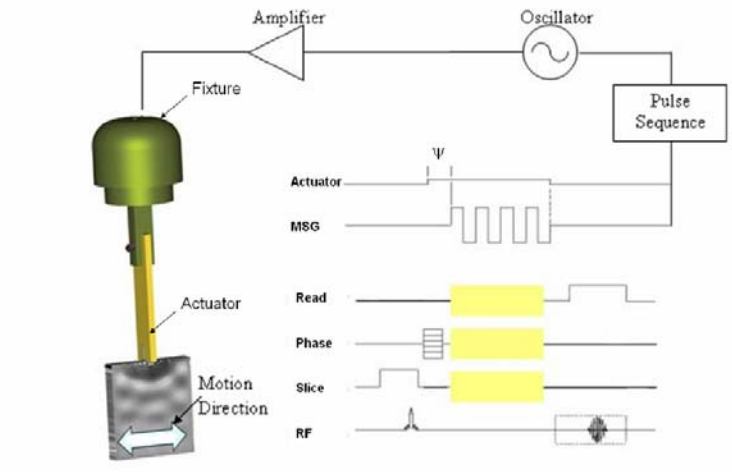

Results

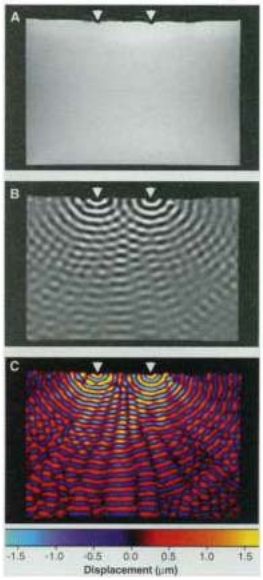

A➔B: Phase difference imaging

B➔C: $\phi(\mathbf{r},\boldsymbol{\theta}) = \gamma \int_0^{\tau=NT<TE} \vec{G}_r(t).\vec{\xi}_0.\cos(\mathbf{k}.\mathbf{r} - \omega t + \boldsymbol{\theta})dt$

$$= \frac{2\gamma NT(\mathbf{G}_r.\vec{\xi}_0)}{\pi}.\sin(\mathbf{k}.\mathbf{r} + \boldsymbol{\theta})$$

Fig. 2. Propagating shear waves. (**A**) Spin-echo MR image showing a uniform tissue-simulating gel object measuring 20 cm transversely. Acoustic shear wave excitation (500 Hz) was applied at two discrete points (arrowheads) separated by 54 mm, with the transverse motion of 2 μm directed perpendicular to the image plane. (**B**) The strain-wave imaging sequence illustrated in Fig. 1 was used with the harmonic motion-sensitizing gradient (20 cycles) directed perpendicular to the image plane. This phase image demonstrates a pattern of phase shifts corresponding to shear waves propagating from each source. Various wave properties such as wavelength and attenuation are depicted, as well as a classic dual-source interference pattern with regions where phase shifts add constructively and destructively. (**C**) Using Eq. 5, we converted the phase shifts (A) to displacement values encoded in a color scale to emphasize the quantitative nature of the method.

C➔ Material Properties: μ

$$c_s = \sqrt{\frac{2}{\rho}\frac{\mu_1^2 + (2\pi f)^2\mu_2^2}{\mu_1 + \sqrt{\mu_1^2 + (2\pi f)^2\mu_2^2}}}$$

$$\delta = \frac{4\pi^2 f\mu_2}{\mu_1 + \sqrt{\mu_1^2 + (2\pi f\mu_2)^2}}$$

Results

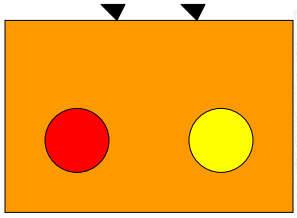

- A simulating gel object, two cylindrical gel inserts with different shear modulus are embedded inside.
  - Red represents stiffer gel with respect to main object
  - Yellow represents softer gel insert

Fig. 4. Magnetic resonance elastography. A tissue-simulating gel object containing two embedded gel cylinders (dotted lines, 44-mm diameter) with differing stiffness was imaged. Shear-wave excitation at 250 Hz (perpendicular to the image plane) with a lateral-displacement amplitude of 5.0 μm was applied to a wide contact plate on the surface. (**A**) This NMR displacement image demonstrates planar shear waves propagating down from the surface. The cylinder on the left is stiffer than the surrounding gel, resulting in a wavelength larger than that in surrounding gel. Conversely, the wavelength in the softer gel cylinder on the right is shorter than that in surrounding gel. The image also demonstrates refraction phenomena, causing a focusing effect within the softer cylinder. (**B**) Quantitative map of shear modulus (μ_{MR}) computed from the local wavelength of the displacement image. The NMR-estimated shear modulus of the plug on the left, for instance, is ~22 kN/m², in good agreement with earlier measurements of large homogeneous samples of the same gel (23.8 kN/m²).

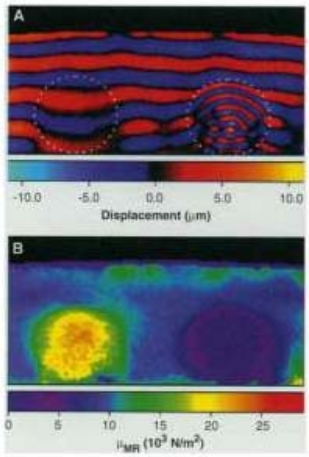

Results

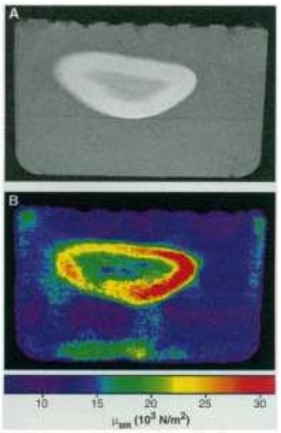

Fig. 5. Porcine kidney. (**A**) Conventional gradient echo image of a fresh kidney specimen embedded in gel demonstrates renal cortex surrounding renal medulla. (**B**) MR elastogram computed from wavelength data averaged from four images each at 200- and 400-Hz shear-wave excitation. The superficial layer of the cortex has a shear modulus of 21 to 30 kN/m^2, distinctly higher than that of the medulla.

- Porcine kidney:
  - Excitation with 200 and 400 Hz
  - The surrounding gel, superficial layer of cortex and the inner medium of the kidney can be easily distinguished.
- In this experiment it is assessed that shear waves with displacement of less than 100nm can be observed.

Results

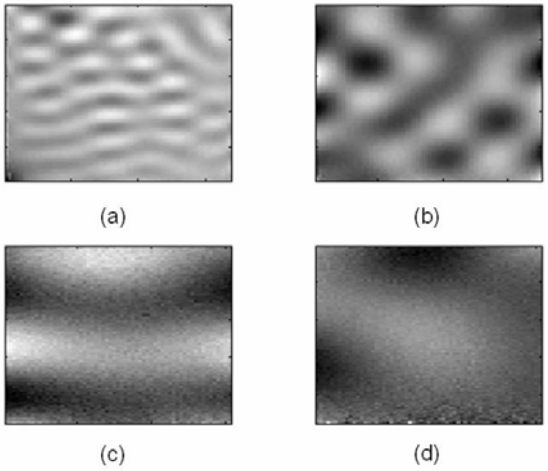

- Shear wave images in homogenous phantoms with different stiffness, agar concentration (%w):
  - (a) 0.25
  - (b) 0.5
  - (c) 0.75
  - (d) 1
- Mechanical excitation frequency = 550 Hz
- FOV = 1.2cm
- in plane resolution = 93.75μm x 93.75μm
- slice thickness = 500 μm

Results

Table 1. Relaxation times for agar gel tested using μMRE and the corresponding mechanical properties. Driving frequency of the mechanical actuator was 550 Hz.

Gel concentration (% wt.)	0.25	0.5	0.75
T1 (ms)	2360	2160	2170
T2 (ms)	91.7	74	87
Wavelength λ_s (mm)	1.7	4.1	5.5
Shear wave speed c_s (m/s)	0.88	2.2	3
Log decrement δ	0.37	0.7	0.82
Shear stiffness (kPa)	0.77	4.84	9.15
Shear elasticity $\mu 1$ (kPa)	0.857	4.89	8.69
Shear viscosity $\mu 2$ (Pa-s)	0.029	0.32	0.67

Recent & Future Work

- In all the work presented the shear waves are generated at the surface of the object using an electromechanical driver.
  - Disadvantage: shear waves are heavily attenuated by tissue and may not reach deeper structures of interest.
  - The problem can be solved to some extend by increasing the surface actuation amplitude and using higher amplitude motion encoding gradients.
- Ideal: shear waves created deep within a object
  - Focused Ultra-Sound

Recent & Future Work

- Focused Ultra-Sound Tranducer

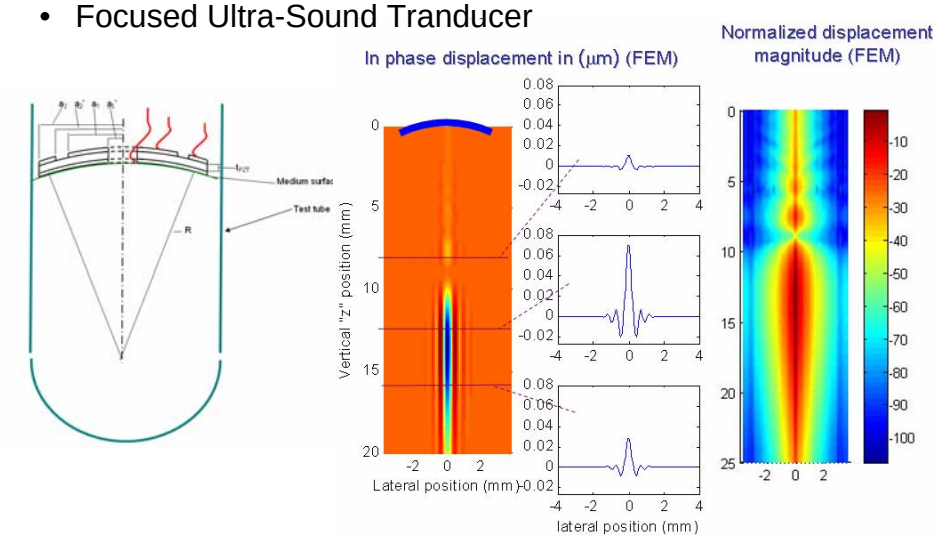

References

- Magnetic Resonance Elastography by Direct Visualization of Propagating Acoustic Strain Waves. R. Muthupillai, D.J. Lomas, P.J. Rossman, J.F. Greenleaf, A. Manduca, R.L. Ehman - Science, 1995
- Magnetic Resonance Imaging of Transverse Acoustic Strain Waves. R. Muthupillai, P.J. Rossman, D.J. Lomas, J.F. Greenleaf, S.J. Riederer, R.L. Ehman – Magnetic Resonance in Medicine, 1996
- Ophir J, Cespedes I, Ponnekanti H, Yazdi Y, Li X. Elastography: a quantitative method for imaging the elasticity of biological tissues. Ultrasonic imaging 1991;13:111-134.
- Plewes D.B, Betty I, Urchuk S.N, Soutar I: Visualizing Tissue Compliance with MR Imaging – JMRI 1995
- Hamhaber U, Grieshaber F. A, Nagel J.H, Klose U: Comparison of Quantitative Shear Wave MR – Elastography with Mechanical Compression Tests - Magnetic Resonance in Medicine, 2003
- Bernstein MA, King KF, Zhou XJ. Handbook of MRI Pulse Sequences. Elsevier Academic Press 2004.
- Fung Y.C: A First Course in Continuum Mechanics, Prentice HallInc. 1994
- Othman S. F, Huihui X, Royston T.J, Magin R.L: Microscopic Magnetic Resonance Elastography - Magnetic Resonance in Medicine, 2005